

OXYGEN-17 AND PROTON MR MICROSCOPY IN MATERIALS ANALYSIS

G.D. MATEESCU,[†] R.A. KINSEY[‡] AND G.M. YVARIS[†][†]Department of Chemistry, Case Western Reserve University
Cleveland, Ohio 44106, USA

and

[‡]B.F. Goodrich Research & Development Center
Brecksville, Ohio 44141 USA

ABSTRACT

Preliminary results of two applications of $^{17}\text{O}/^1\text{H}$ NMR microimaging ($\text{MR}\mu\text{I}$) are described. In the first case, it is shown that oxygen-17 $\text{MR}\mu\text{I}$ presents a unique advantage in situations where a strong proton background hinders the analysis of water ingress in polymeric materials. This is illustrated with ^{17}O -enriched water diffusion into an agar gel from a central well. While proton imaging cannot readily distinguish between exogenous and endogenous water, ^{17}O imaging makes a clear differentiation, due to the fact that the natural abundance gel has virtually no ^{17}O background. In the second case, proton $\text{MR}\mu\text{I}$ was used to analyze the structure and performance of commercial time-release pellets (ProMac^R) containing an active ingredient (surfactant) dispersed into an inert matrix. This was done after leaching the detergent with natural abundance water or after drying the leached sample and refilling the pores with water. Pores ranging in size from 25 to 325 μm diameter are clearly visualized. The ^1H images have been quantitated with commercial image analysis software in terms of the total porosity and the individual pore characteristics. Two types of water can be separately imaged: "bound" water with restricted mobility (interacting with the polymer matrix), and "free" water (in large pools). The majority of water is in the bound state. It is possible to evaluate the control-release performance of the product from the size of the pores, the uniformity of dispersion and the time course of detergent-water exchange.

INTRODUCTION

The oxygen-17 nucleus is generally regarded as "unfavorable" for NMR experiments for two principal reasons: quadrupolar line broadening and very low natural abundance. Until recently, its use in MR imaging has not even been considered.

However, the feasibility of ^{17}O MRI and localized spectroscopy has been demonstrated during the past three years. Indeed, it has been shown¹⁻¹¹ that the "unfavorable" magnetic resonance properties of ^{17}O can actually be turned into advantages: the fast relaxation allows much shorter pulse intervals than with proton, and even modest isotopic enrichment dramatically increases the signal-to-contrast ratio. Thus, an enrichment of 3.7 atom % increases the concentration by a factor of 100 and decreases the measurement time by a factor of 10,000. In fact, in vivo detection of local (mouse brain) concentrations as low as 0.5% H_2^{17}O has been recently reported.⁹

The low gamma of ^{17}O leads to the necessity of increasing the gradient strength by a factor of 7.37 (the $\gamma_{\text{H}}/\gamma_{\text{O}}$ ratio) in

order to achieve a resolution comparable to that of proton MRI. This is quite feasible with high performance NMR instruments generally employed for materials characterization.

Perhaps, the most important attribute of ^{17}O MRI resides in the possibility to detect labeled water molecules in a large pool of water. This opens a unique avenue towards precise determination of net transport of water in systems that naturally contain water and/or mobile protons (e.g., elastomers, biopolymers, etc). The specific example presented in this communication refers to migration of water through an agar gel.

With regard to proton imaging, it is shown here that an adequate resolution can be obtained by employing small sample size in a microscope accessory attached to a high performance NMR system. This is illustrated by the measurement of pore sizes in a ProMac^R material,¹² a low density polyethylene (LDPE) coextruded with a surfactant (LAS, linear alkylbenzene sulfonate) to form a time-release system.¹² The surfactant is a bactericide used to enhance the reclamation of land after surface mining. It inhibits the growth of acid-producing bacteria which hinder revegetation.

MATERIALS AND METHODS

Oxygen-17 and proton images were obtained on a Bruker MSL 400 system equipped with a double resonance ($^{17}\text{O}/^1\text{H}$) microimaging probe which also incorporates the gradient coils. Gradient strengths in excess of 100 Gauss/cm can be obtained. Proton spectra were taken with a Bruker AM-200 instrument.

NMR micrographs were taken employing two kinds of spin warp sequences: one with a soft 90° (single lobe sinc) pulse for slice selection followed by a hard 180° pulse, in order to obtain short echo times (TE) for imaging of "bound" water; the other, with both soft pulses, for imaging "free" water. Specific parameters are given in the text or in Figure captions.

Oxygen-17 enriched (40 atom %) water was purchased from the Monsanto-Mound laboratories. Natural abundance water was distilled and deionized.

The agar gel (0.7%) was prepared with hot (80 °C) water, poured in two identical 18 mm I.D. NMR tubes, each containing a concentric 5 mm O.D. tube. After cooling, the 5 mm tubes were removed to obtain the wells in which the natural abundance or ^{17}O -labeled water was placed at the beginning of each diffusion experiment.

Two kinds of ProMac^R (42.5 % LAS)/LDPE rods were investigated: one having a 7 mm diameter (PRO1) and the other having a 4 mm diameter (PRO2).

A rod of PRO1, 2 cm long, was extracted by stirring in 600 ml of distilled water at ambient temperature for 10 days. The water was changed twice a day. After removing external excess water with filter paper, the leached sample was imaged for both bound and free water. A control consisting of unleached PRO1 was wrapped in wet filter paper in order to show that, in our conditions, both the surfactant (LAS) and LDPE did not yield an image.

After leaching, rods of PRO2 were dried in the oven at 70 °C. They were then placed in NMR tubes containing a quantity of water which was approximately twice the volume of the rod. The tubes were sealed and kept in a bath at 70 °C for 20 hours. Since there was very little indication of water ingress

the tubes were removed from the bath and stored 100 days at room temperature to allow completion of the diffusion process. The samples were imaged after removal of excess external water with filter paper. All images were performed in 10 mm inserts.

The percent porosity and pore size parameters (length, width, area, perimeter, shape function) were determined using the stored image analysis (SIA) software on a Tracor Northern Energy Dispersive X-ray Analyzer.

RESULTS AND DISCUSSION

Water Diffusion in Agar Gel

A comparison of proton and oxygen-17 images taken at the beginning and the end of parallel studies of water transport within a mass of agar gel is shown in Figure 1. It is obvious

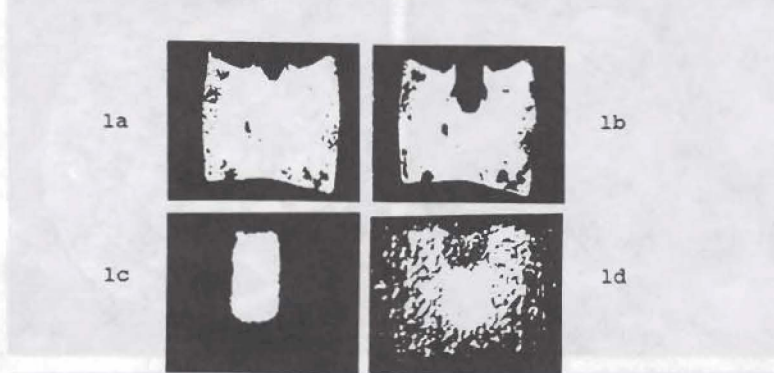


Figure 1. a&b: proton images of a 500 μm slice through the agar gel phantom described in the Materials and Methods section. A spin warp sequence with soft 90 and 180° pulses was employed with echo times (TE) of 12 ms, field of view 26 mm and 113 $\mu\text{m}/\text{pixel}$ resolution. a: Image taken approximately one hour after gel preparation and adding natural abundance water in the central well; time of repetition (TR) 1s, total experiment time (ET) = 8 min. b: Image after 20 hr; ET = 16 min. c&d: oxygen-17 images of a similar phantom as above, but after adding 5 atom % ^{17}O -water in the central well. A hard 180° pulse was used to shorten the echo time. c: image at five minutes. d: image at 108 minutes. TE = 2 ms, TR = 28 ms, ET = 4 min, ST = 14 mm, resolution 157 $\mu\text{m}/\text{pixel}$.

that the evaluation of a diffusion coefficient from proton data is virtually impossible. In dramatic contrast, the ^{17}O images provide unambiguous data for the calculation of H_2O diffusion. Work is in progress for the adaptation of Fick's law to three dimensional NMR determination of the diffusion coefficient. Performing parallel experiments with D_2O will contribute to the understanding of this complicated process. We emphasize here the strong difference between the behavior of oxygen and hydrogen as representatives of a given water molecule. Indeed, while oxygen will be permanently attached to the originally labeled molecule, hydrogen or deuterium will be rapidly separated from it by intermolecular exchange processes.

Proton MR Microscopy of Porous Polyethylene

In preparation for MR μ I, one dimensional ^1H spectroscopy was performed on the samples. Initial attempts to hydrate ProMac^R rods for study of the water or surfactant were unsuccessful. After equilibration to a relative humidity of 74% a broad featureless line is observed with a linewidth of ~ 1300 Hz. There is no chemical shift resolution, so this signal may be from either water or surfactant. Attempts were made to induce proton mobility by raising the temperature. At 90°C the linewidth was 430 Hz. These preparations were not judged to yield samples suitable for imaging.

Exchanging the LAS for water by soaking the material in water for ten days yielded 200 Hz (water) linewidths. A small

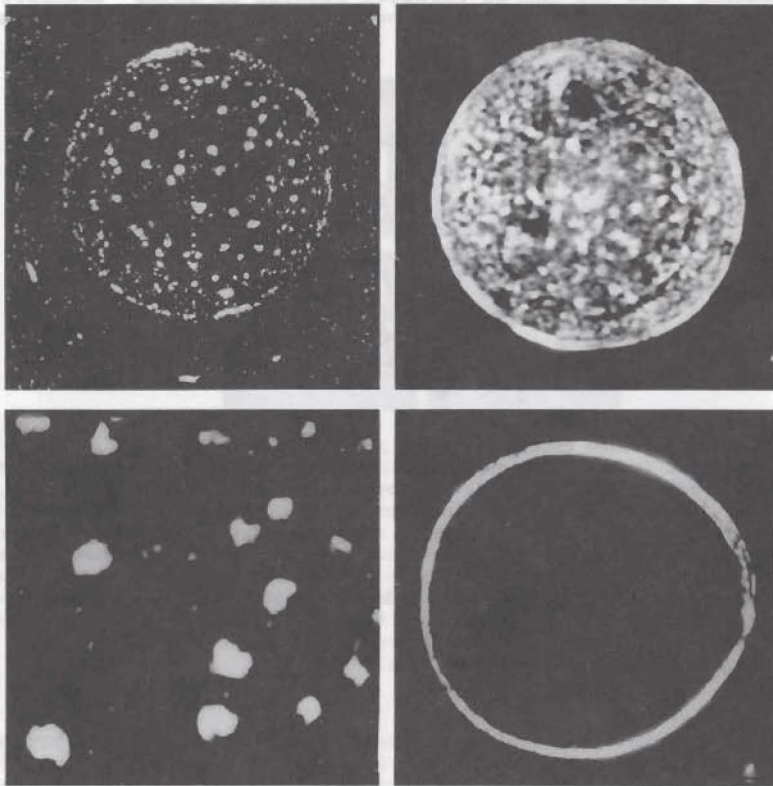


Figure 2

shoulder at high field was detected. This could be interpreted either as a susceptibility effect or as due to residual surfactant. The water that fills the voids left by the leached LAS constitutes the source of signal for imaging.

Figure 2 (upper left) shows a transverse NMR microimage yielded by the leached LDPE (7 mm diameter, $300\ \mu\text{m}$ slice

thickness). The in-plane pixel resolution is $10\mu\text{m}$. The echo time (TE=6 ms) was adjusted to emphasize the free water in "large" pores. This image indicates there are no significant areas devoid of signal, and hence a uniform surfactant distribution.

An image emphasizing the bound water (TE=3ms) is shown in Figure 2 (upper right). Again, the pixel resolution is $10\mu\text{m}$ and the slice thickness is $300\mu\text{m}$. This image was taken of a rod wrapped in filter paper which absorbed excess water at the exterior of the sample, thus defining its perimeter. The bound water covers nearly the entire cross section except for several areas, the largest ($\sim 800\mu\text{m}$) being situated on the left side, close to the horizontal diameter. Careful examination of the image reveals a circular feature without water, particularly visible in the upper two quadrants which could be interpreted as a result of the extrusion process.

Figure 2 (lower right) shows a slice through a control (unexchanged) LDPE rod wrapped in wet filter paper. No signal appears in the interior due to lack of visible water and immobility of the LAS and LDPE protons.

PRO2 samples (not shown here) revealed a more dense pore distribution which corresponds to a much slower (hence, efficient) LAS release. Indeed, it took up to 100 days to extract the surfactant.

Image Analysis

The lower left of Figure 2 represents an expansion of a small region from the first quadrant of the image above. This area was scanned and digitized into a binary image by a Tracor Northern energy dispersive x-ray analyzer. As with comparing images, care must be taken when adjusting the image threshold for the digitization. Stored Image Analysis (SIA) software allows for quantitative evaluation of the pores. Each pore is defined in terms of location, diameter, length, width, area, perimeter, and orientation. Averages of each of these parameters are calculated as well as total porosity (the percentage of area covered by pores). Histograms can be produced for the distribution of the pore parameters. The calculated porosity of this region is 8.3%. The particles range in diameter from 25-300 μm within two major pore size distributions, 25-70 and 170-300 μm .

Table I. Characteristics for Pores Larger than 100 μm

Part.	Av.diam.	Area	Perim.	Cntr-x	Cntr-y	Length	Width
1	100	8,700	340	140	90	130	100
2	180	23,440	580	1,900	130	200	160
3	170	23,070	560	610	270	200	150
4	230	38,630	730	1,160	280	270	200
5	210	28,210	670	750	490	220	190
6	285	57,160	910	1,560	600	310	250
7	170	17,420	550	160	660	220	110
8	270	53,360	880	1,970	700	290	250
9	210	27,690	650	140	1,350	220	180
10	260	49,940	840	890	1,440	290	220
11	198	23,820	620	60	1,780	240	130
12	300	63,490	960	2,070	1,750	350	270

However, pores smaller than 70 μm may be indistinguishable

from noise. Table I contains data for the pores larger than 70 μm in diameter.

CONCLUSIONS

When a proton background hinders the ^1H MRI analysis of diffusion of water in a polymeric system, employing ^{17}O -enriched water and ^{17}O MRI brings an elegant and efficient solution. Use of other ^{17}O labeled liquids (alcohols, phenols, ethers etc.), is also deemed possible.

Proton microscopy of porous materials constitutes a valuable means for characterization of inner structures, voids and defects. Exploiting differences in relaxation parameters results in establishing the extent of tight or weak interactions between the matrix and the incorporated liquid. In addition, determining the time course of water (or other solvent) ingress is an invaluable means to evaluate the performance of time-release products.

ACKNOWLEDGMENTS. We thank A.A. Sobek and J.B. Pausch for useful discussions and J.J. Bacskay for performing the water-LAS exchanges. We acknowledge R.W. Smith for doing the image analysis.

NOTES AND REFERENCES

1. G.D. Mateescu and Terri Dular, Oxygen-17 NMR Imaging, ENC (Experimental NMR Conference) 28, 73a (1987).
2. G.D. Mateescu, G.M. Yvars and T. Dular, Oxygen-17 MRI, Soc. Magn. Res. Med. (SMRM), 6, 929a. (1987).
3. G.D. Mateescu, G. Yvars, D. Pazara and N. Alldridge, $^{17}\text{O}/^1\text{H}$ NMR Microscopy, ENC, 29, 189, (1988).
4. G.D. Mateescu, G.M. Yvars, D. Pazara, J. LaManna, D. Lust, K. McCracken, M. Mattingly and W. Kuhn, Oxygen-17: A Physiological, Biochemical and Anatomical MRI Contrast Agent, SMRM 7, 600 (1988).
5. G.D. Mateescu, G.M. Yvars and Terri Dular, Water, Ions and ^{17}O MRI, Water and Ions in Biological Systems, edited by P. Lauger (Birkhauser Publishers, Basel, 1988), p.239-250.
6. G.D. Mateescu, G.M. Yvars, D.I. Pazara, N.A. Alldridge, J.C. LaManna, W.D. Lust, M. Mattingly and W. Kuhn, Combined $^{17}\text{O}/^1\text{H}$ MR Microscopy in Plants, Animals and Materials, Synthesis and Applications of Isotopically Labeled Compounds, Baillie & Jones, Eds. (Elsevier, 1989) 499-508.
7. G.D. Mateescu, G. Yvars, L. Maylish-Kogovsek, J. LaManna, W.D. Lust and D. Sudilovsky, ^{17}O MRI and MRS of the Brain, the Heart and Coronary Arteries, SMRM 8, 859 (1989).
8. G.D. Mateescu and G.M. Yvars, Oxygen-17 MR Imaging: Theory and Experiment, ENC 30, 197a (1989).
9. G.D. Mateescu, G. M. Yvars, J.C. LaManna, W.D. Lust and D. Sudilovsky, Oxygen-17 MRS: in vivo Evaluation of Water Uptake and Residence Time in the Mouse Brain after Injection of $\text{O}-17$ Labeled Water, SMRM 9, 1236 (1990).
10. G.D. Mateescu, G.M. Yvars, J.C. LaManna, D.W. Lust and D. Sudilovsky, Volume selected ^{17}O Spectroscopy in Experimental Cerebral Ischemia, ENC, 31, 205a (1990).
11. G.D. Mateescu, Oxygen-17 Imaging of Non-Biological Materials, FACSS 17, 427a (1990).
12. a) ProMac is a registered trade mark of E.F. Goodrich Co.
b) A.A. Sobek, D.A. Benedetti, V.J. Rastogi, Proc. Mining and Reclamation Conf., Vol. 1, 33-42 (1990).